

**New Alkali Lanthanide-free Polyoxometalates with Remarkable Water-
Responsive Turn-Off-On Luminescence Properties**

Aurély Bagghi, Rania Ghena, Nicolas Gautier, Nicolas Stephan, Philippe Deniard,* Rémi
Dessapt*

Nantes Université, CNRS, Institut des Matériaux de Nantes Jean Rouxel, IMN, F-44000
Nantes, France

Electronic Supporting Information

Table of contents:

Fig. S1- Experimental and simulated PXRD patterns of $\text{Na}_7[\text{SbW}_6\text{O}_{24}]\cdot16\text{H}_2\text{O}$ and $\text{K}_5\text{Na}_2[\text{SbW}_6\text{O}_{24}]\cdot12\text{H}_2\text{O}$	4
Fig. S2- Experimental and simulated PXRD patterns of $\text{K}_7[\text{SbW}_6\text{O}_{24}]\cdot6\text{H}_2\text{O}$	5
Fig. S3- FT-IR spectra of $\text{Na}_7[\text{SbW}_6\text{O}_{24}]\cdot16\text{H}_2\text{O}$, $\text{K}_5\text{Na}_2[\text{SbW}_6\text{O}_{24}]\cdot12\text{H}_2\text{O}$ and $\text{K}_7[\text{SbW}_6\text{O}_{24}]\cdot6\text{H}_2\text{O}$	6
Fig. S4- High Angle Annular Dark Field image, EDS spectrum and EDS ratio acquired on $\text{K}_7[\text{SbW}_6\text{O}_{24}]\cdot6\text{H}_2\text{O}$	7
Fig. S5- Crystal packing of $\text{Na}_7[\text{SbW}_6\text{O}_{24}]\cdot16\text{H}_2\text{O}$	8
Fig. S6- TGA/DSC curves of $\text{K}_5\text{Na}_2[\text{SbW}_6\text{O}_{24}]\cdot12\text{H}_2\text{O}$	9
Fig. S7- TGA/DSC curves of $\text{K}_7[\text{SbW}_6\text{O}_{24}]\cdot6\text{H}_2\text{O}$	10
Fig. S8- PXRD patterns of $\text{Na}_7[\text{SbW}_6\text{O}_{24}]$, $\text{K}_5\text{Na}_2[\text{SbW}_6\text{O}_{24}]$ and $\text{K}_7[\text{SbW}_6\text{O}_{24}]$	11
Table S1- Crystallographic data and structure refinement parameters of $\text{K}_5\text{Na}_2[\text{SbW}_6\text{O}_{24}]$... Fig. S9- Observed, refined and difference patterns of $\text{K}_5\text{Na}_2[\text{SbW}_6\text{O}_{24}]$ after Rietveld refinement at 500 °C.....	12
Table S2- Crystallographic data and structure refinement parameters of $\text{K}_7[\text{SbW}_6\text{O}_{24}]$ Fig. S10- Observed, refined and difference patterns of $\text{K}_7[\text{SbW}_6\text{O}_{24}]$ after Rietveld refinement (T = 30 °C).....	13
Fig. S11- FTIR-ATR spectra of $\text{K}_5\text{Na}_2[\text{SbW}_6\text{O}_{24}]$ and $\text{K}_7[\text{SbW}_6\text{O}_{24}]$	14
Fig. S12- FT-Raman spectra of $\text{K}_5\text{Na}_2[\text{SbW}_6\text{O}_{24}]$ and $\text{K}_7[\text{SbW}_6\text{O}_{24}]$	15
Fig. S13- TGA/DSC curves of rehydrated $\text{Na}_7[\text{SbW}_6\text{O}_{24}]$	16
Fig. S14- PXRD patterns of rehydrated $\text{K}_5\text{Na}_2[\text{SbW}_6\text{O}_{24}]$ and $\text{K}_7[\text{SbW}_6\text{O}_{24}]$	17
Fig. S15- Evolution of the PXRD pattern of $\text{Na}_7[\text{SbW}_6\text{O}_{24}]\cdot16\text{H}_2\text{O}$ during successive dehydration (200°C)/rehydration (100% RH, room temperature, 3 days) cycles.....	18
Fig. S16- SEM images of $\text{K}_5\text{Na}_2[\text{SbW}_6\text{O}_{24}]\cdot12\text{H}_2\text{O}$ and $\text{K}_5\text{Na}_2[\text{SbW}_6\text{O}_{24}]$ particles during a thermal dehydration (200 °C, 10 minutes)/rehydration (100% RH, 3 days) process.....	19
Fig. S17- PXRD pattern of deuterated $\text{K}_5\text{Na}_2[\text{SbW}_6\text{O}_{24}]$	20
Fig. S18- FTIR-ATR spectrum of deuterated $\text{K}_5\text{Na}_2[\text{SbW}_6\text{O}_{24}]$	21
Fig. S19- Absorption spectra of $\text{Na}_7[\text{SbW}_6\text{O}_{24}]\cdot16\text{H}_2\text{O}$, $\text{Na}_7[\text{SbW}_6\text{O}_{24}]$, $\text{K}_5\text{Na}_2[\text{SbW}_6\text{O}_{24}]\cdot12\text{H}_2\text{O}$, $\text{K}_5\text{Na}_2[\text{SbW}_6\text{O}_{24}]$, $\text{K}_7[\text{SbW}_6\text{O}_{24}]\cdot6\text{H}_2\text{O}$ and $\text{K}_7[\text{SbW}_6\text{O}_{24}]$	22
Fig. S20- Room-temperature excitation and emission spectra of $\text{Na}_7[\text{SbW}_6\text{O}_{24}]\cdot16\text{H}_2\text{O}$, $\text{K}_5\text{Na}_2[\text{SbW}_6\text{O}_{24}]\cdot12\text{H}_2\text{O}$ and $\text{K}_7[\text{SbW}_6\text{O}_{24}]\cdot6\text{H}_2\text{O}$	23
Fig. S21- CIE chromaticity diagrams of $\text{Na}_7[\text{SbW}_6\text{O}_{24}]\cdot16\text{H}_2\text{O}$, $\text{K}_5\text{Na}_2[\text{SbW}_6\text{O}_{24}]\cdot12\text{H}_2\text{O}$ and $\text{K}_7[\text{SbW}_6\text{O}_{24}]\cdot6\text{H}_2\text{O}$	24
Fig. S22- Room-temperature luminescence decay curves of $\text{Na}_7[\text{SbW}_6\text{O}_{24}]\cdot16\text{H}_2\text{O}$, $\text{Na}_7[\text{SbW}_6\text{O}_{24}]$, $\text{K}_5\text{Na}_2[\text{SbW}_6\text{O}_{24}]\cdot12\text{H}_2\text{O}$, $\text{K}_5\text{Na}_2[\text{SbW}_6\text{O}_{24}]$, $\text{K}_7[\text{SbW}_6\text{O}_{24}]\cdot6\text{H}_2\text{O}$ and $\text{K}_7[\text{SbW}_6\text{O}_{24}]$	25

Fig. S23- Room-temperature emission spectrum and decay curve of deuterated $\text{K}_5\text{Na}_2[\text{SbW}_6\text{O}_{24}]$	26
Fig. S24- Room-temperature excitation and emission spectra of $\text{K}_5\text{Na}_2[\text{SbW}_6\text{O}_{24}]$ and $\text{K}_7[\text{SbW}_6\text{O}_{24}]$	27
Fig. S25- CIE chromaticity diagrams of $\text{Na}_7[\text{SbW}_6\text{O}_{24}]$, $\text{K}_5\text{Na}_2[\text{SbW}_6\text{O}_{24}]$ and $\text{K}_7[\text{SbW}_6\text{O}_{24}]$	28
Fig. S26- Room-temperature emission spectra of $\text{K}_5\text{Na}_2[\text{SbW}_6\text{O}_{24}]\cdot12\text{H}_2\text{O}$ and $\text{K}_7[\text{SbW}_6\text{O}_{24}]\cdot6\text{H}_2\text{O}$ during a dehydration/rehydration cycle.....	29
Fig. S27- Evolution of the room-temperature PL spectra (monitored at 254 nm) upon exposure to 100% RH over a period of 480 min for (a) $\text{Na}_7[\text{SbW}_6\text{O}_{24}]$, and over a period of 120 min for (b) $\text{K}_5\text{Na}_2[\text{SbW}_6\text{O}_{24}]$ and (c) $\text{K}_7[\text{SbW}_6\text{O}_{24}]$	30
Fig. S28- PXRD patterns of $\text{K}_5\text{Na}_2[\text{SbW}_6\text{O}_{24}]\cdot12\text{H}_2\text{O}$ and $\text{K}_5\text{Na}_2[\text{SbW}_6\text{O}_{24}]$ after rehydration (1h at 100% RH)	31
References	32

Fig. S1. Comparison between experimental (red line) and simulated (black line) PXRD patterns of a) $\text{Na}_7[\text{SbW}_6\text{O}_{24}]\cdot16\text{H}_2\text{O}$, and b) $\text{K}_5\text{Na}_2[\text{SbW}_6\text{O}_{24}]\cdot12\text{H}_2\text{O}$.

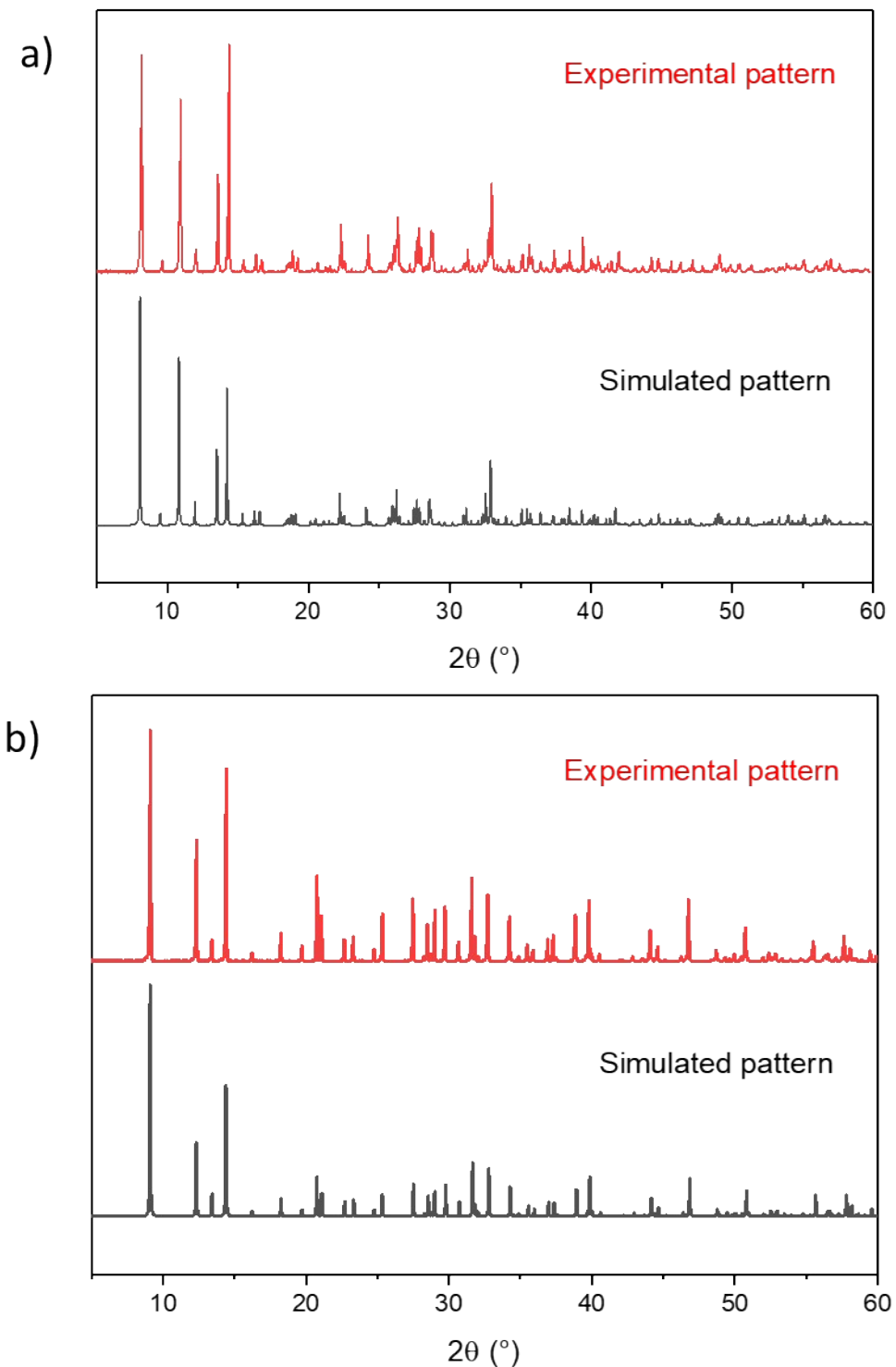


Fig. S2. Comparison between the experimental PXRD pattern of $\mathbf{K}_7[\text{SbW}_6\text{O}_{24}]\cdot 6\text{H}_2\text{O}$ (red line) and the simulated PXRD pattern of the reported $\mathbf{K}_{5.5}\text{H}_{1.5}[\text{SbW}_6\text{O}_{24}]\cdot 6\text{H}_2\text{O}^{\text{S}1}$ compound (black line).

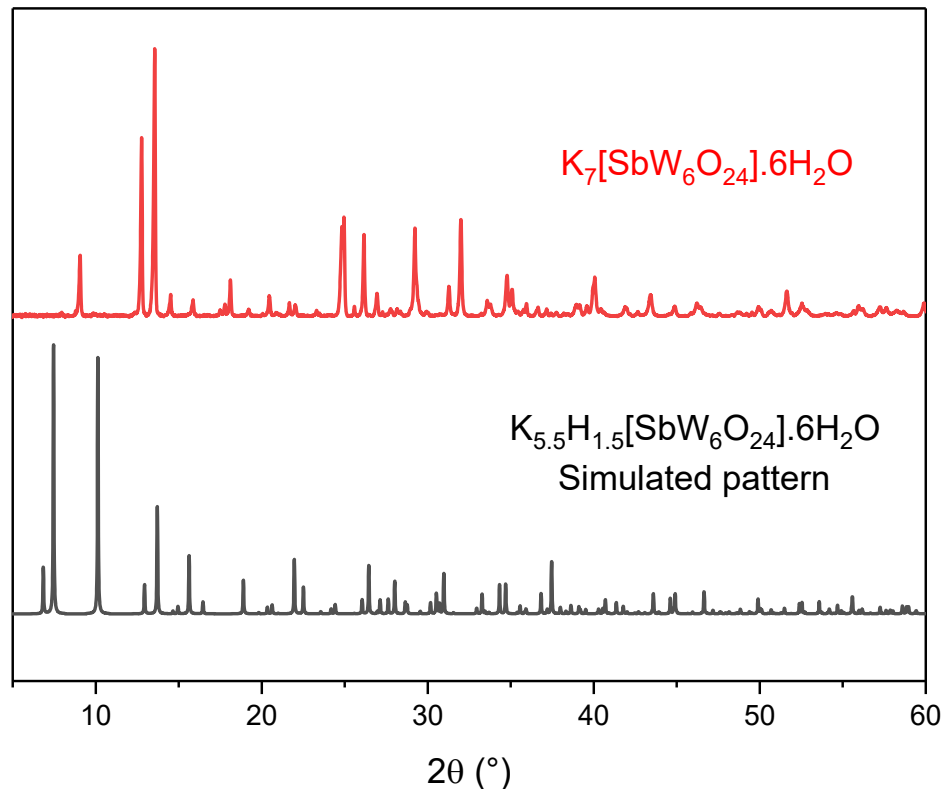


Fig. S3. Comparison of the FT-IR spectra of a) $\text{Na}_7[\text{SbW}_6\text{O}_{24}]\cdot16\text{H}_2\text{O}$ (black line), b) $\text{K}_5\text{Na}_2[\text{SbW}_6\text{O}_{24}]\cdot12\text{H}_2\text{O}$ (red line), and c) $\text{K}_7[\text{SbW}_6\text{O}_{24}]\cdot6\text{H}_2\text{O}$ (blue line).

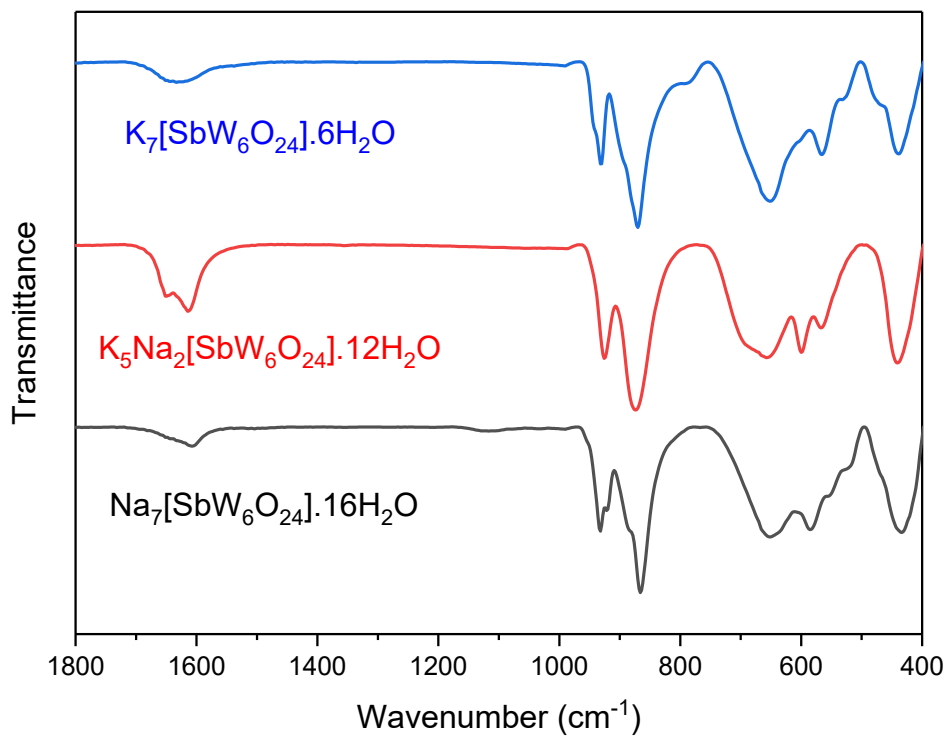
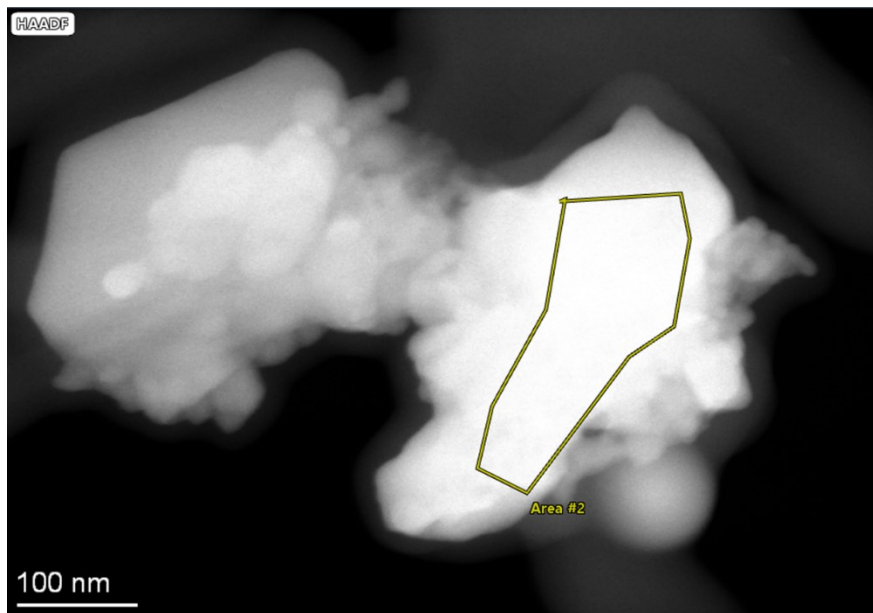
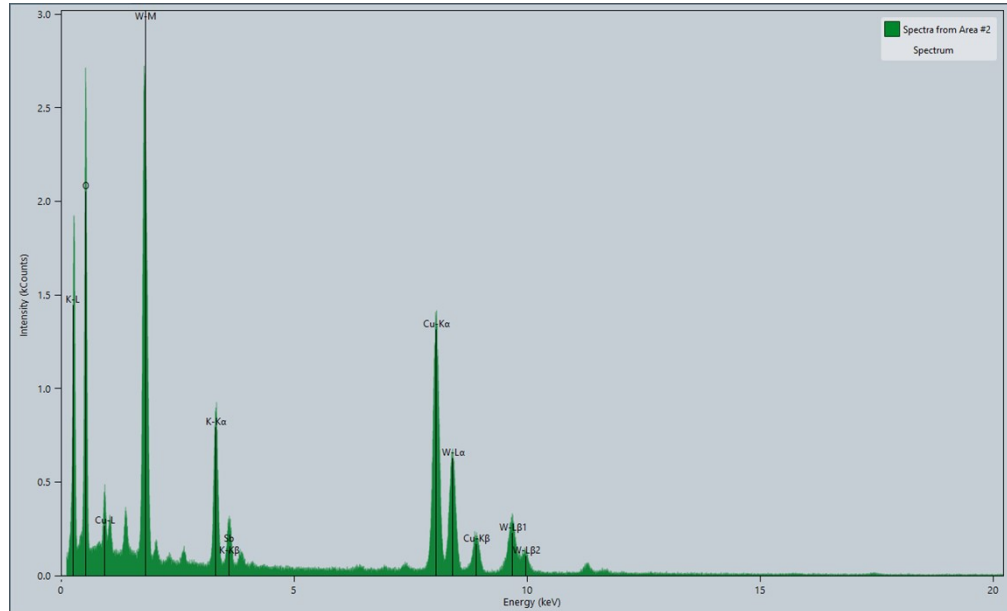


Fig. S4. a) High Angle Annular Dark Field image, b) EDS spectrum and c) EDS ratio acquired on $\text{K}_7[\text{SbW}_6\text{O}_{24}]\cdot 6\text{H}_2\text{O}$.

a)



b)



c)

Element	Atomic %	Ratio
Sb	7.17	1
W	43.35	6
K	49.48	6.9

Fig. S5. Representation of the complex H-bonding network involving the $[\text{SbW}_6\text{O}_{24}]^{7-}$ unit and water molecules in $\text{Na}_7[\text{SbW}_6\text{O}_{24}]\cdot 16\text{H}_2\text{O}$ (grey octahedra = WO_6 , pink octahedra = SbO_6 ,

green octahedra = NaO_6 , orange sphere: oxygen atoms of the POM unit, blue sphere: oxygen atoms of water molecules. H-bonding interactions between the POM anion and water molecules are displayed as blue dotted lines. H atoms are not displayed.

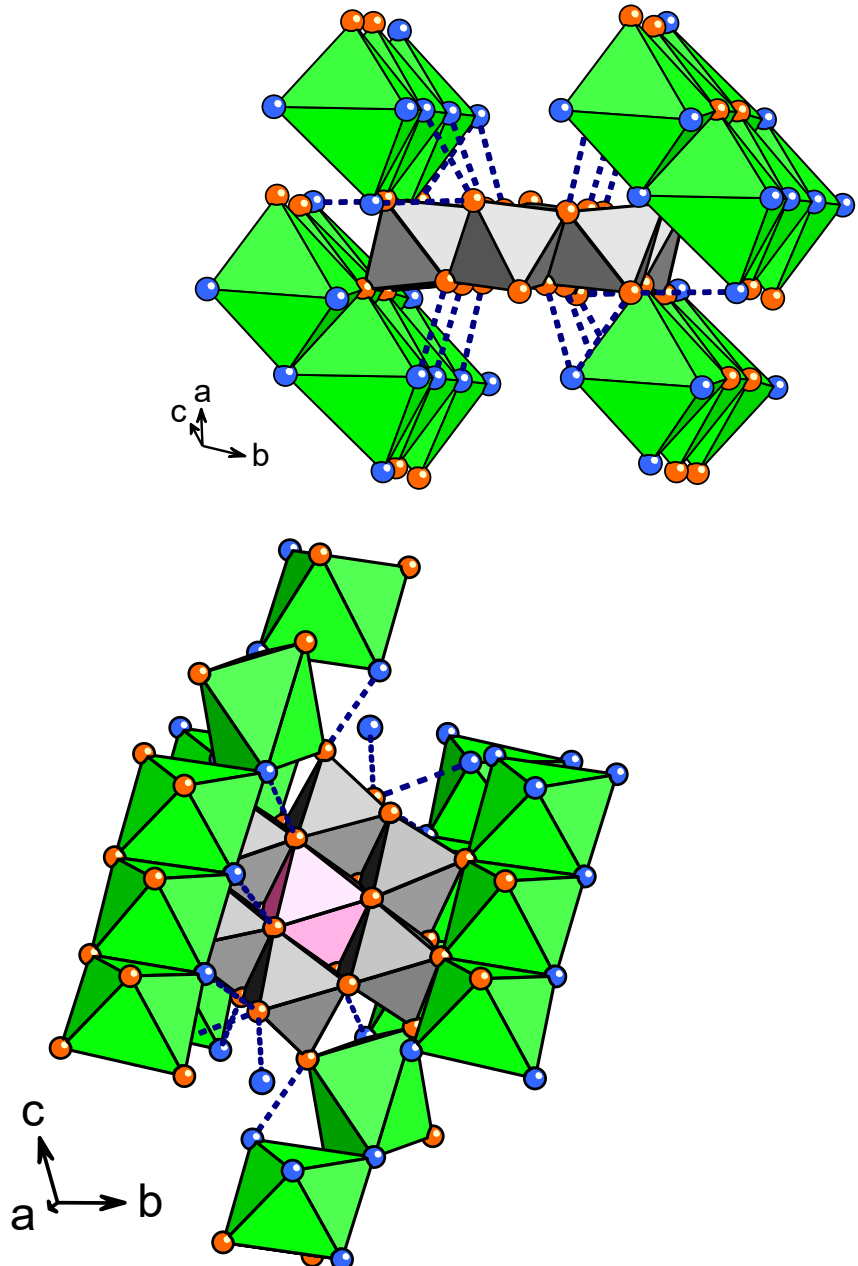
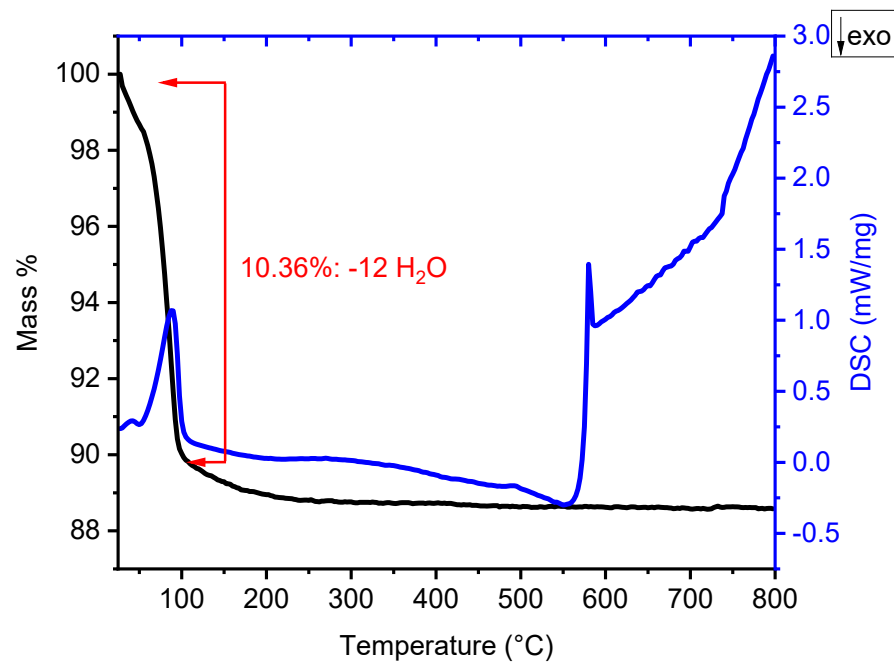
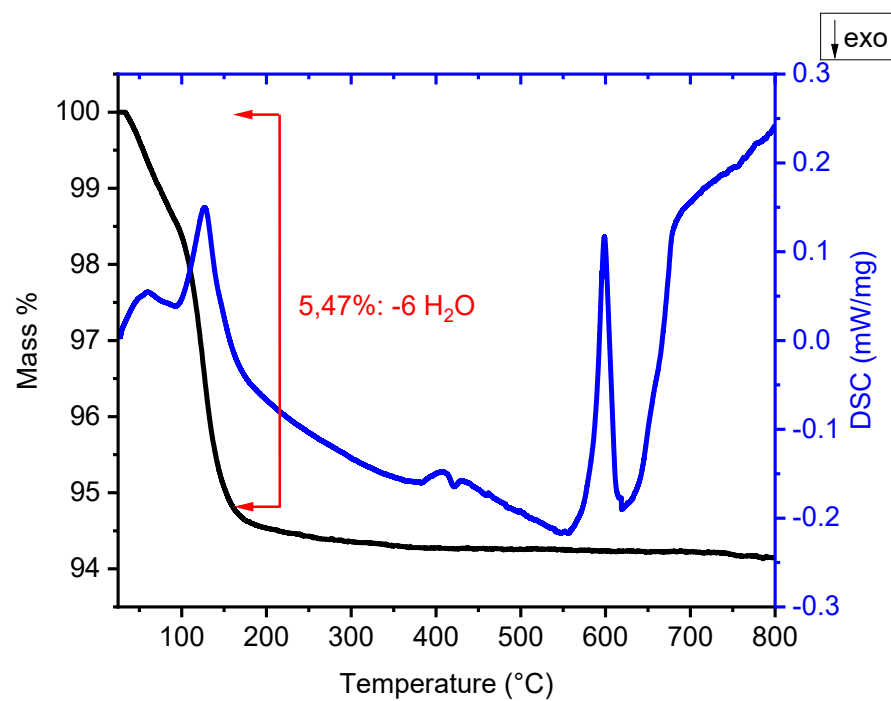


Fig. S6. TGA (black line) and DSC (blue line) curves of $\mathbf{K_5Na_2[SbW_6O_{24}] \cdot 12H_2O}$.



The TGA/DSC curves show a weight loss of 10.36 % in the temperature range of 25-115 °C characterized by a sharp endothermic peak, in well agreement with the full removal of twelves water molecules (theoretical mass loss = 10.45 %).

Fig. S7. TGA (black line) and DSC (blue line) curves of $\mathbf{K}_7[\mathbf{SbW}_6\mathbf{O}_{24}]\cdot 6\mathbf{H}_2\mathbf{O}$.



The TGA/DSC curves show a weight loss of 5.47 % in the temperature range of 25-175 °C characterized by a sharp endothermic peak, in well agreement with the full removal of six water molecules (theoretical mass loss = 5.43 %).

Fig. S8. PXRD patterns of $\text{Na}_7[\text{SbW}_6\text{O}_{24}]$ (blue line), $\text{K}_5\text{Na}_2[\text{SbW}_6\text{O}_{24}]$ (red line) and $\text{K}_7[\text{SbW}_6\text{O}_{24}]$ (black line), obtained at 650 °C, 500 °C and 550 °C, respectively.

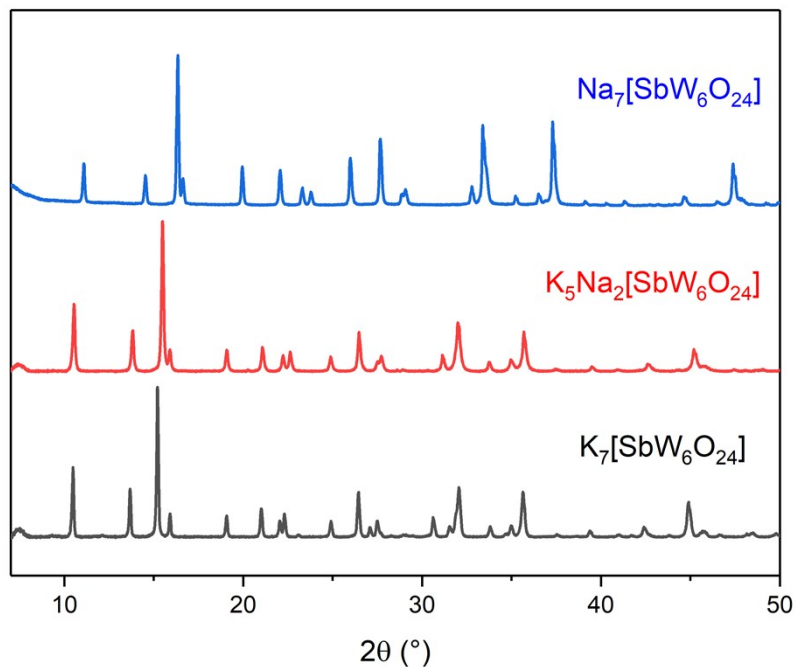


Table S1. Atom positions, site occupation fraction and atomic displacement parameters of $\text{K}_5\text{Na}_2[\text{SbW}_6\text{O}_{24}]$ at 500 °C. High ADP values are due to data collection temperature.

S.G. R^3 , $a(\text{\AA}) = 11.21523(14)$, $c(\text{\AA}) = 17.2672(3)$, $R_{\text{Bragg}} = 6.02$, GOF = 1.66, $R_{\text{wp}} = 8.97$						
atom	x	y	z	SOF	Wyckoff	$U_{\text{iso}} (\text{\AA}^2)$
K1	0	0	0.5	1	3b	0.057(5)
K2	0.1166(12)	0.2508(8)	0.1969(4)	0.72(2)	18f	0.057
Na1	0.1166	0.2508	0.1969	0.28	18f	0.057
O1	0.529(3)	0.1544(18)	0.3854(9)	1	18f	0.039(4)
O2	-0.060(3)	-0.379(3)	0.4010(14)	1	18f	0.039
O3	0.1912(15)	0.107(2)	0.2744(12)	1	18f	0.039
O4	0.202(2)	-0.008(2)	0.4000(11)	1	18f	0.039
Sb1	0	0	0	1	3a	0.018(3)
W1	-0.19144(17)	-0.3306(2)	0.33594(15)	1	18f	0.0271(19)

* $U_{\text{aniso}}(\text{W1})$: 0.026(3); 0.0150(19); 0.0181(12); -0.006(2); 0.005(3); 0.010(2)

Fig. S9. Observed, refined and difference patterns of $\text{K}_5\text{Na}_2[\text{SbW}_6\text{O}_{24}]$ after Rietveld refinement at 500 °C. ($R_{\text{Bragg}} = 6.02$, GOF = 1.66, $R_{\text{wp}} = 8.97$)

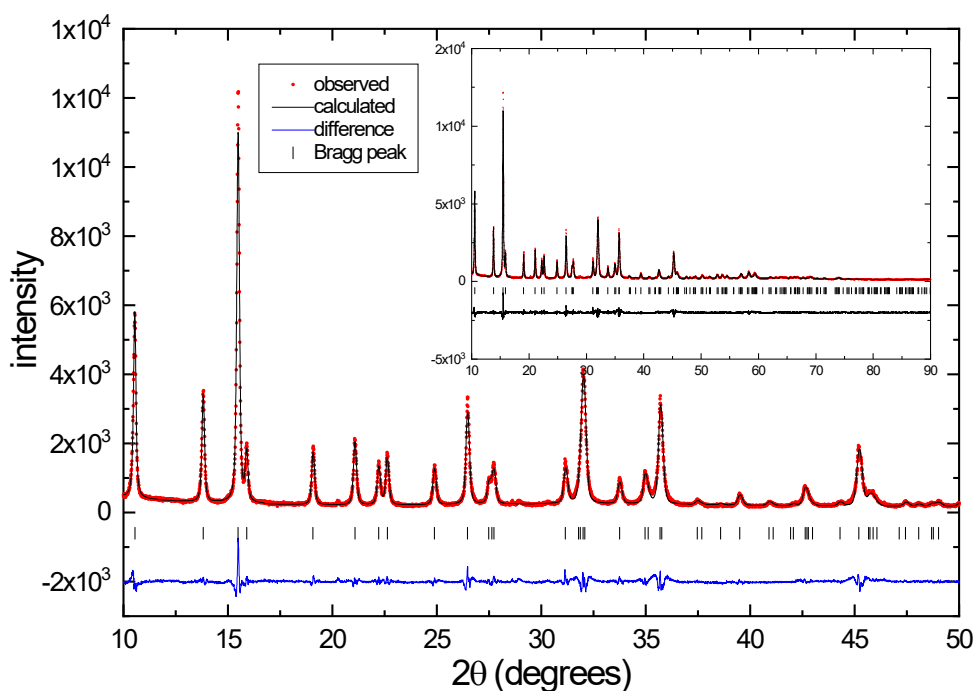


Table S2. Atom positions, site occupation fraction and atomic displacement parameters of $\text{K}_7[\text{SbW}_6\text{O}_{24}]$ at 30 °C.

S.G. $R\bar{3}$, $a(\text{\AA}) = 11.18224(12)$, $c(\text{\AA}) = 17.5388(3)$, $R_{\text{Bragg}} = 2.49$, GOF = 1.31, $R_{\text{wp}} = 7.72$						
atom	x	y	z	SOF	Wyckoff	$U_{\text{iso}} (\text{\AA}^2)$
K1	0	0	0.5	1	3b	0.0466(18)
K2	0.1155(6)	0.2603(4)	0.1933(2)	1	18f	0.0466(18)
O1	0.5241(15)	0.1686(11)	0.3876(6)	1	18f	0.028(2)
O2	-0.0554(15)	-0.3594(15)	0.3886(9)	1	18f	0.028(2)
O3	0.2006(10)	0.1285(13)	0.2716(7)	1	18f	0.028(2)
O4	0.2205(13)	0.0160(16)	0.4010(7)	1	18f	0.028(2)
Sb1	0	0	0	1	3a	0.0168(14)
W1	-0.19003(11)	-0.33030(12)	0.33452(7)	1	18f	0.0197(9)

* $U_{\text{aniso}}(\text{W1})$: 0.0181(13); 0.0187(10); 0.0144(6); 0.0032(13); 0.0033(13); 0.0028(14)

Fig. S10. Observed, refined and difference patterns of $\text{K}_7[\text{SbW}_6\text{O}_{24}]$ after Rietveld refinement (T = 30 °C). ($R_{\text{Bragg}} = 2.49$, GOF = 1.31, $R_{\text{wp}} = 7.72$). The arrows indicate some impurity peaks.

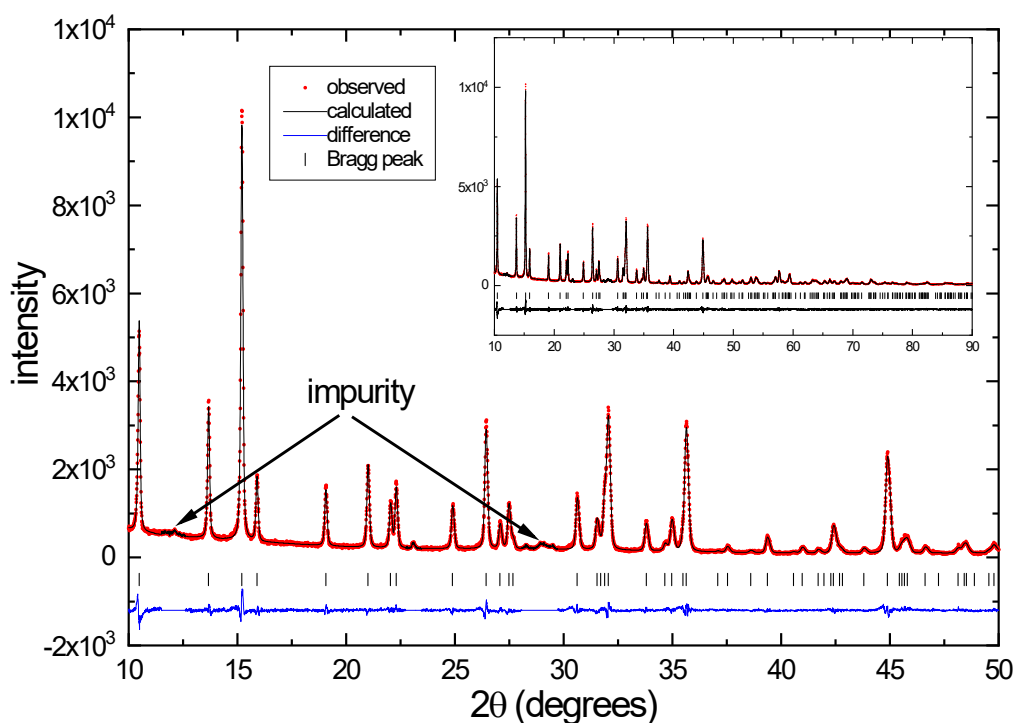


Fig. S11. Comparison of the FTIR-ATR spectra of a) $\text{K}_5\text{Na}_2[\text{SbW}_6\text{O}_{24}]\cdot12\text{H}_2\text{O}$ (black line) and $\text{K}_5\text{Na}_2[\text{SbW}_6\text{O}_{24}]$ (red line), and b) $\text{K}_7[\text{SbW}_6\text{O}_{24}]\cdot16\text{H}_2\text{O}$ (black line) and $\text{K}_7[\text{SbW}_6\text{O}_{24}]$ (red line).

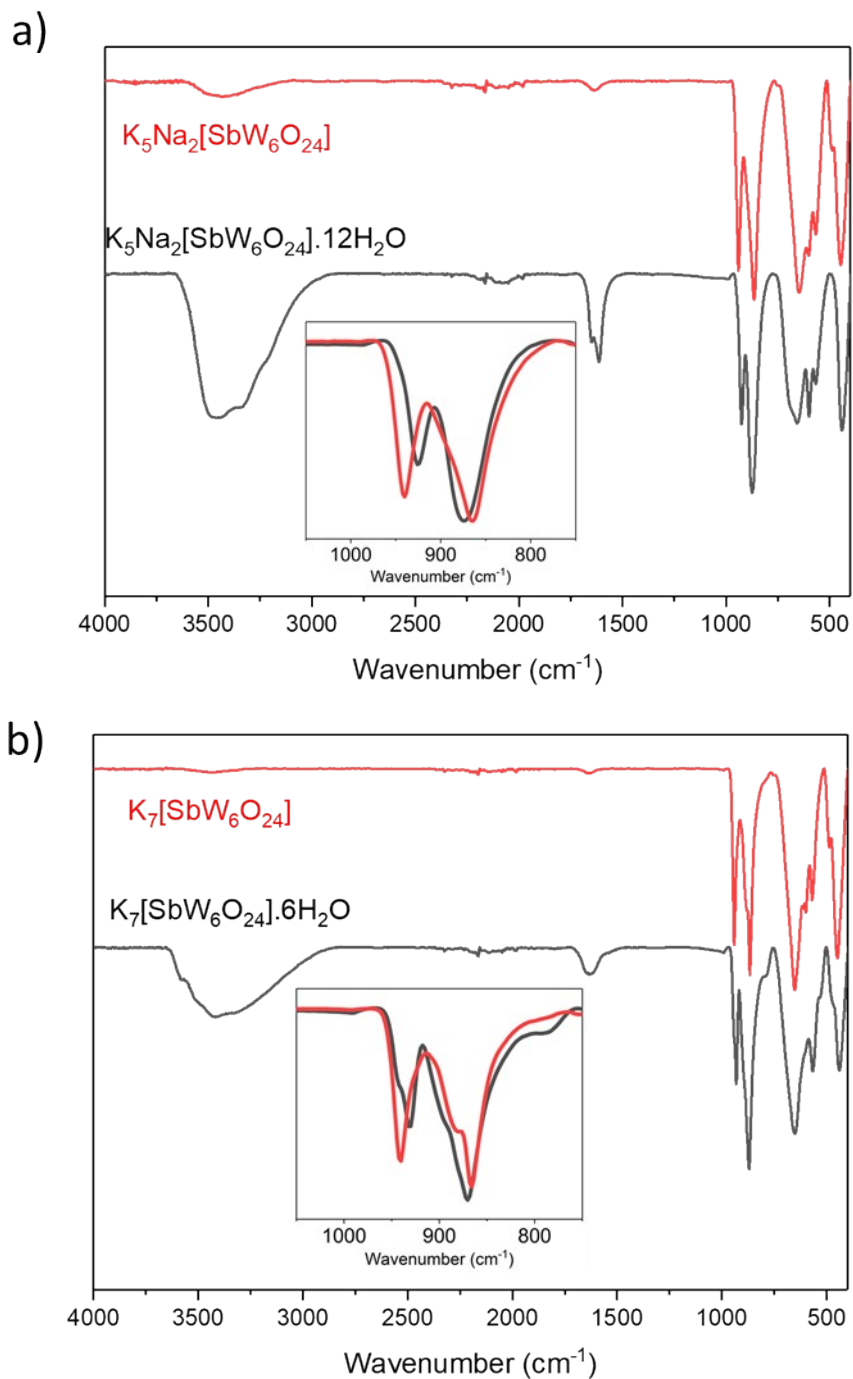


Fig. S12. Comparison of the FT-Raman spectra of a) $\mathbf{K}_5\mathbf{Na}_2[\mathbf{SbW}_6\mathbf{O}_{24}]\cdot12\mathbf{H}_2\mathbf{O}$ (black line) and $\mathbf{K}_5\mathbf{Na}_2[\mathbf{SbW}_6\mathbf{O}_{24}]$ (red line), and b) $\mathbf{K}_7[\mathbf{SbW}_6\mathbf{O}_{24}]\cdot6\mathbf{H}_2\mathbf{O}$ (black line) and $\mathbf{K}_7[\mathbf{SbW}_6\mathbf{O}_{24}]$ (red line).

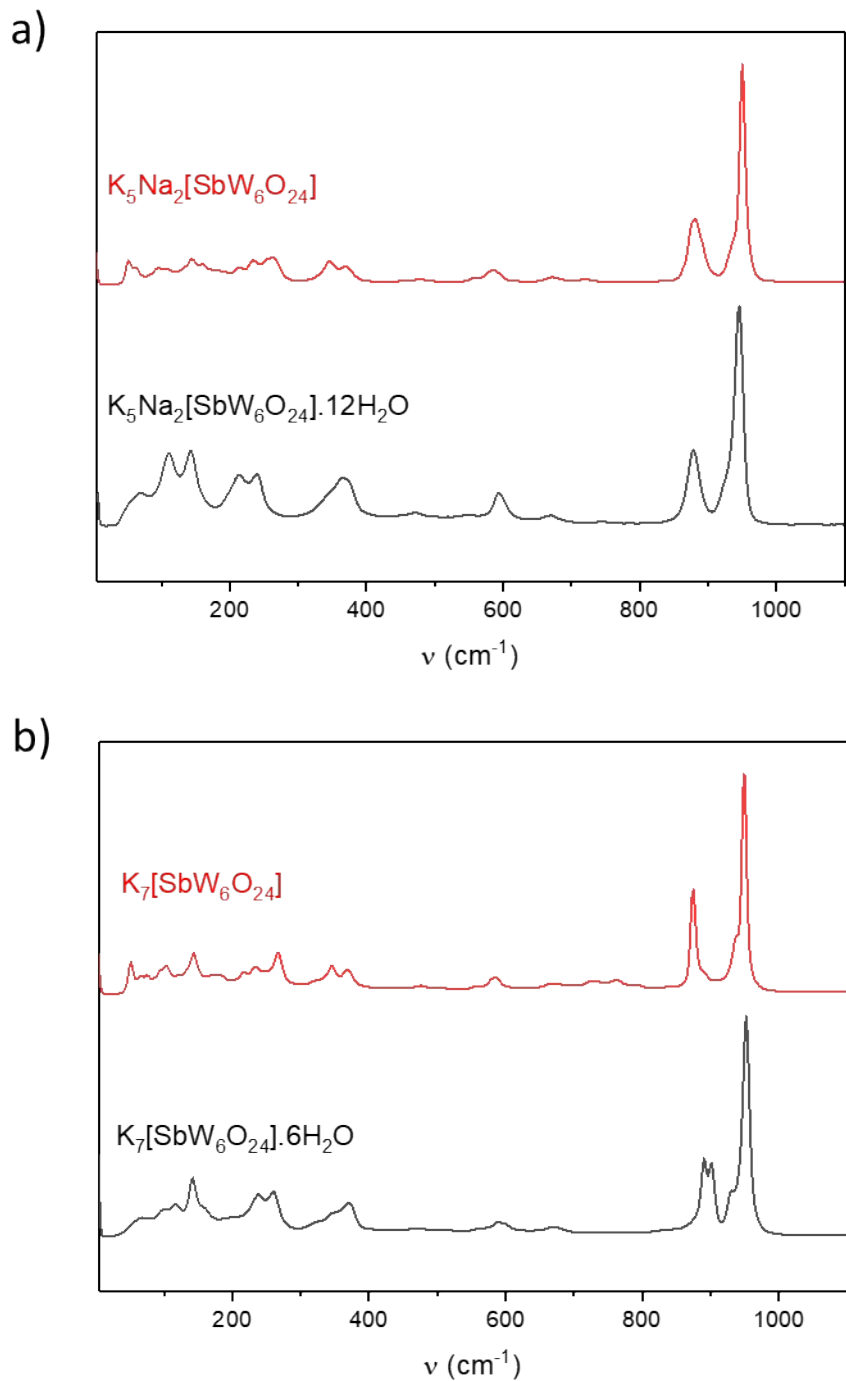


Fig. S13. TGA (black line) and DSC (blue line) curves of $\text{Na}_7[\text{SbW}_6\text{O}_{24}]$ after rehydration in a closed chamber with a relative humidity level (RH%) of 100%, for three days at room temperature.

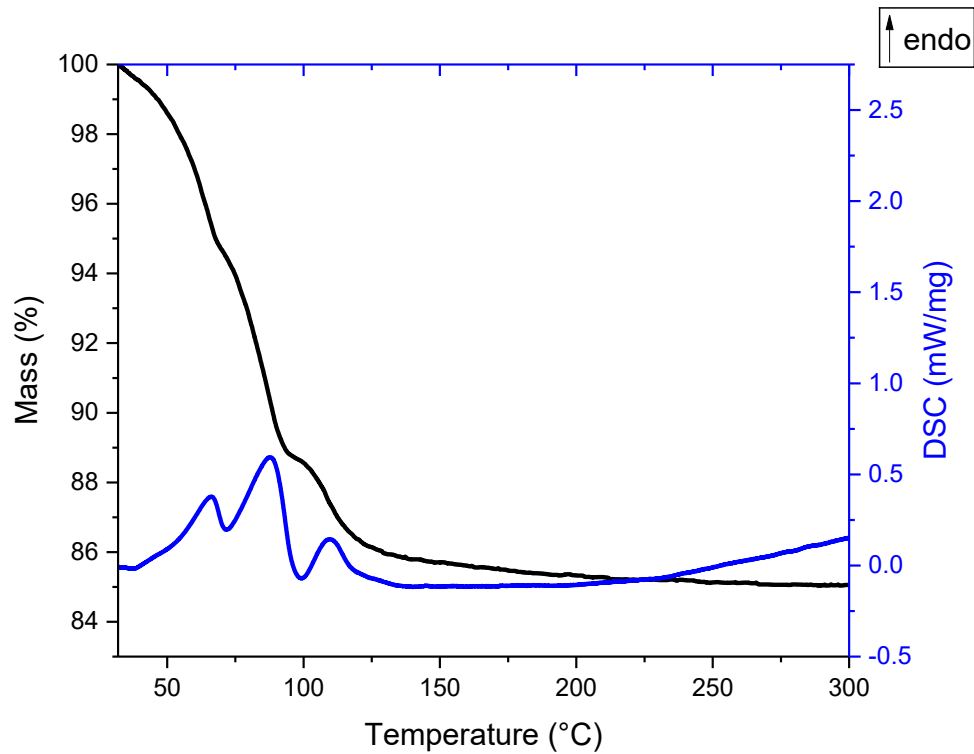


Fig. S14. Comparison of the PXRD patterns of a) $\text{K}_5\text{Na}_2[\text{SbW}_6\text{O}_{24}]\cdot12\text{H}_2\text{O}$ (black line) and $\text{K}_5\text{Na}_2[\text{SbW}_6\text{O}_{24}]$ after rehydration (red line), and b) $\text{K}_7[\text{SbW}_6\text{O}_{24}]\cdot6\text{H}_2\text{O}$ (black line) and $\text{K}_7[\text{SbW}_6\text{O}_{24}]$ after rehydration (red line). For the rehydration process, the anhydrous powdered compounds were kept for three days at room temperature, in a closed chamber with a high relative humidity level (RH%) of 100%.

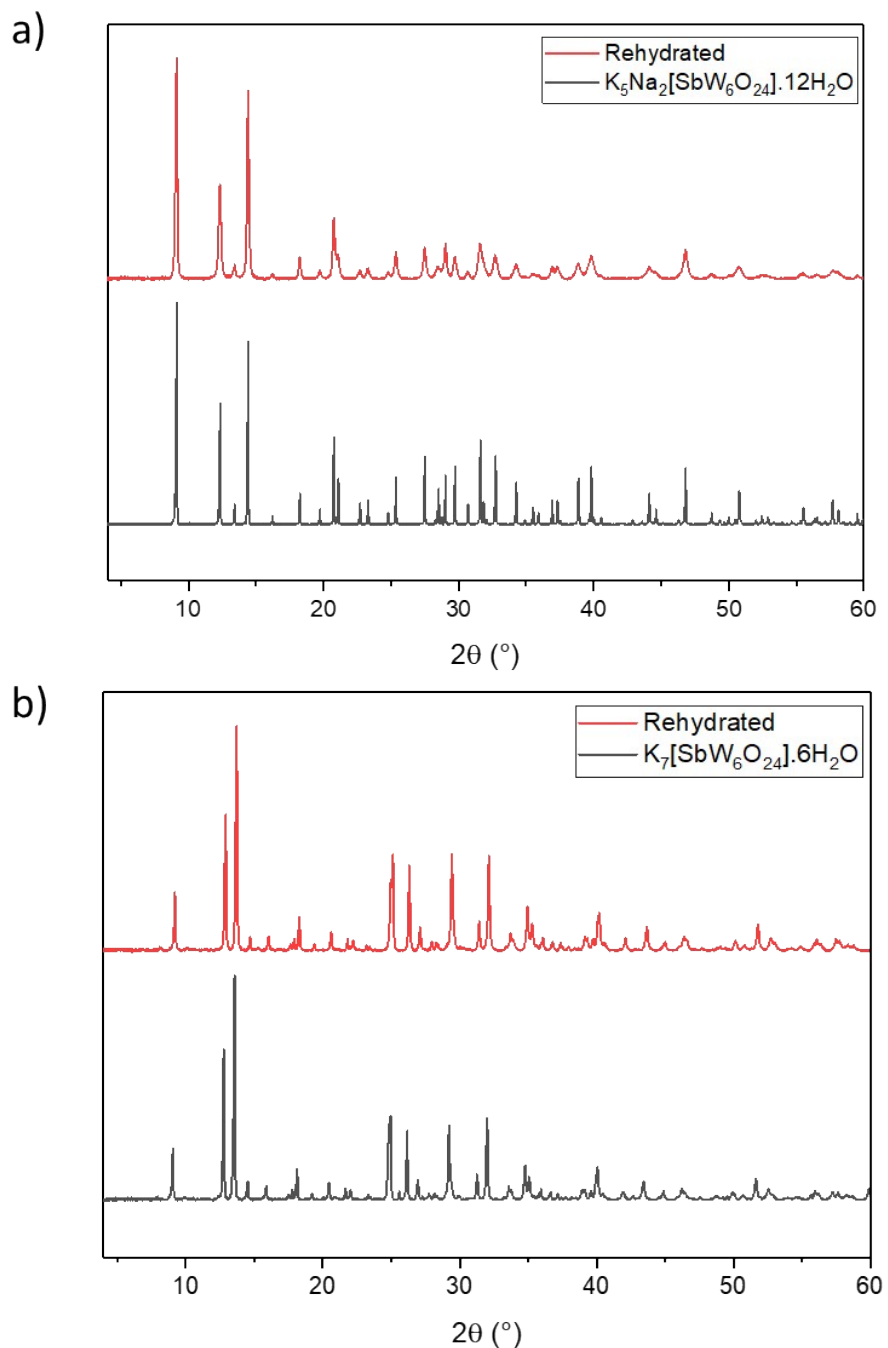


Fig. S15. Evolution of the PXRD pattern of $\text{Na}_7[\text{SbW}_6\text{O}_{24}]\cdot16\text{H}_2\text{O}$ during successive dehydration (200°C)/rehydration (100% RH, room temperature, 3 days) cycles.

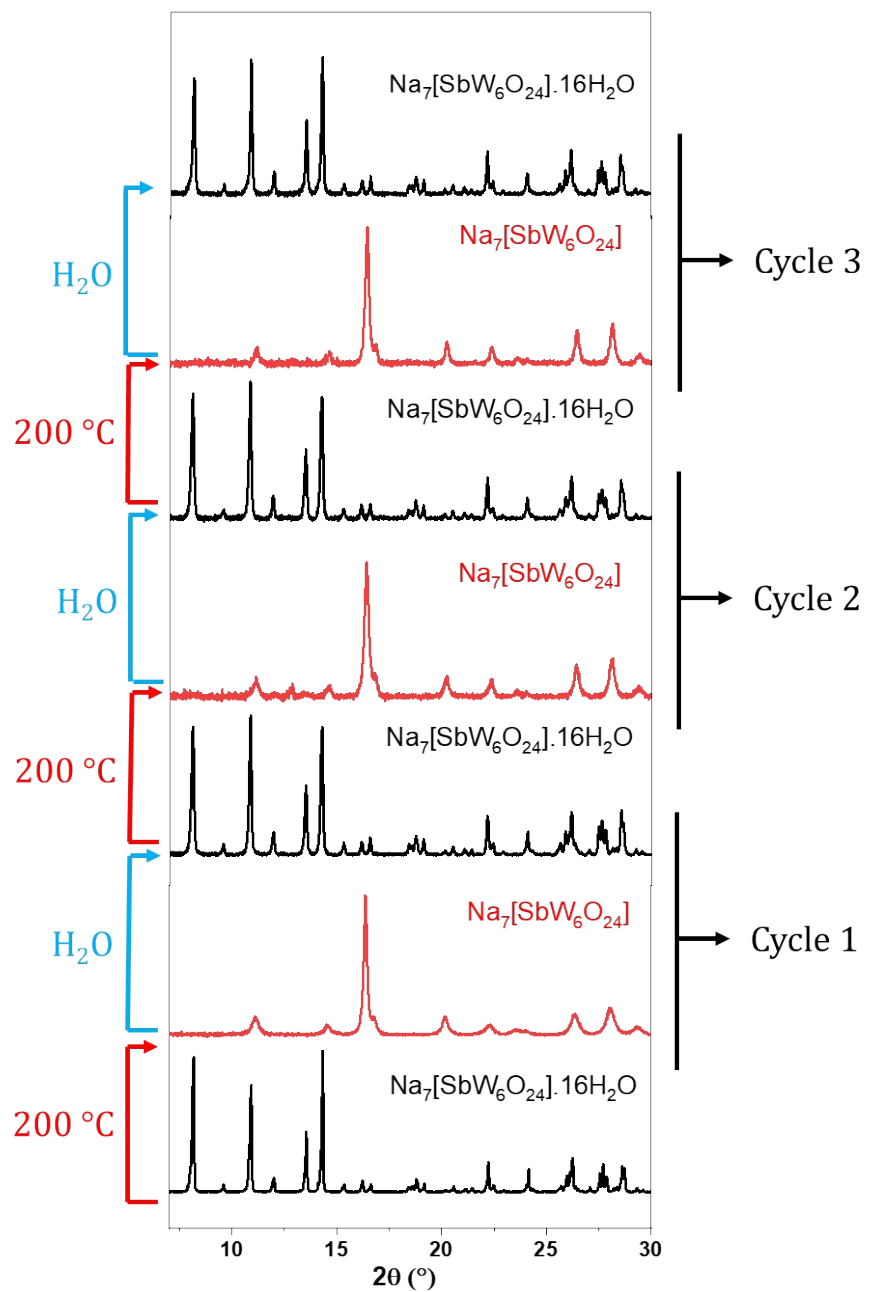


Fig. S16. SEM images of $\text{K}_5\text{Na}_2[\text{SbW}_6\text{O}_{24}]\cdot12\text{H}_2\text{O}$ and $\text{K}_5\text{Na}_2[\text{SbW}_6\text{O}_{24}]$ particles during a thermal dehydration (200°C , 10 minutes)/rehydration (100% RH, 3 days) process.

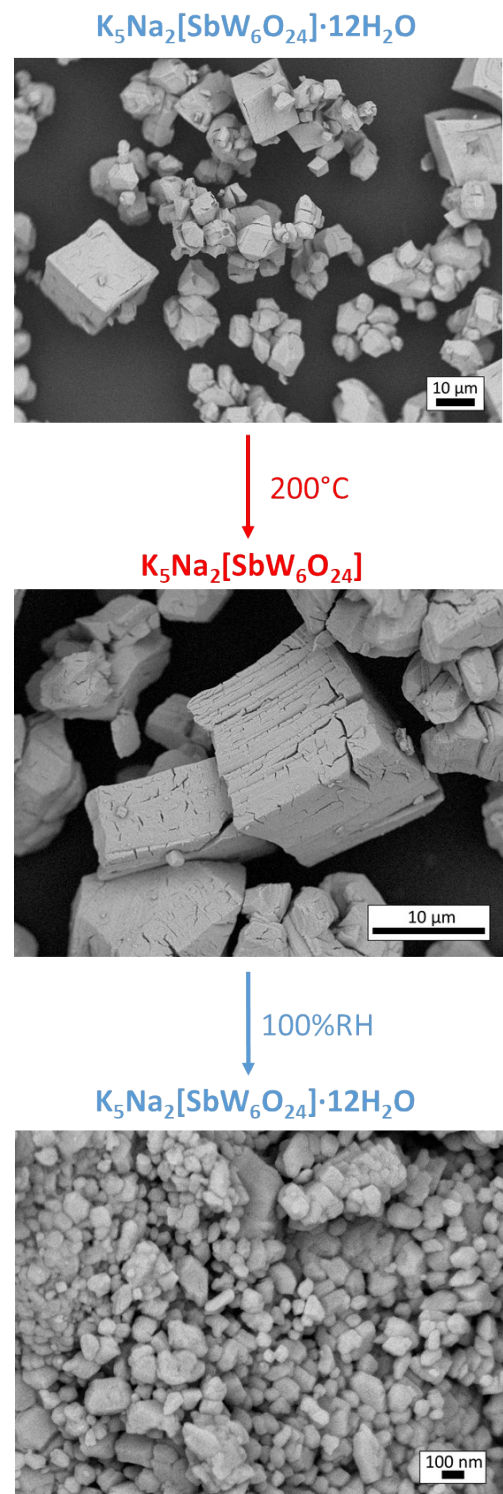


Fig. S17. Comparison of the experimental PXRD pattern of deuterated $\text{K}_5\text{Na}_2[\text{SbW}_6\text{O}_{24}]$ (red line) and the simulated PXRD pattern of $\text{K}_5\text{Na}_2[\text{SbW}_6\text{O}_{24}]\cdot12\text{H}_2\text{O}$ (black line). For the deuteration process, the anhydrous $\text{K}_5\text{Na}_2[\text{SbW}_6\text{O}_{24}]$ powder sample was kept under N_2 atmosphere in a closed chamber containing heavy water, for five days at room temperature.

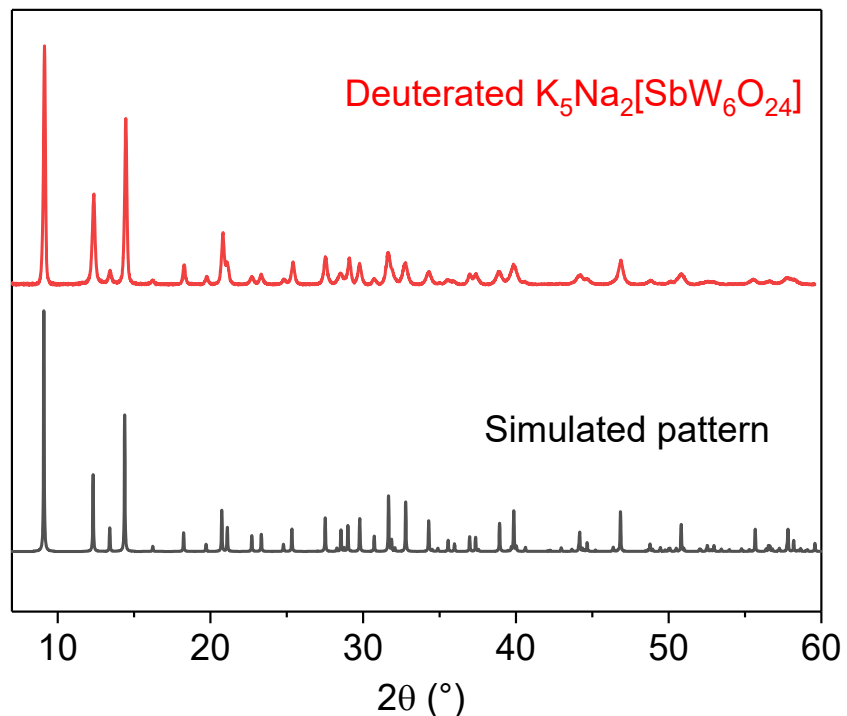
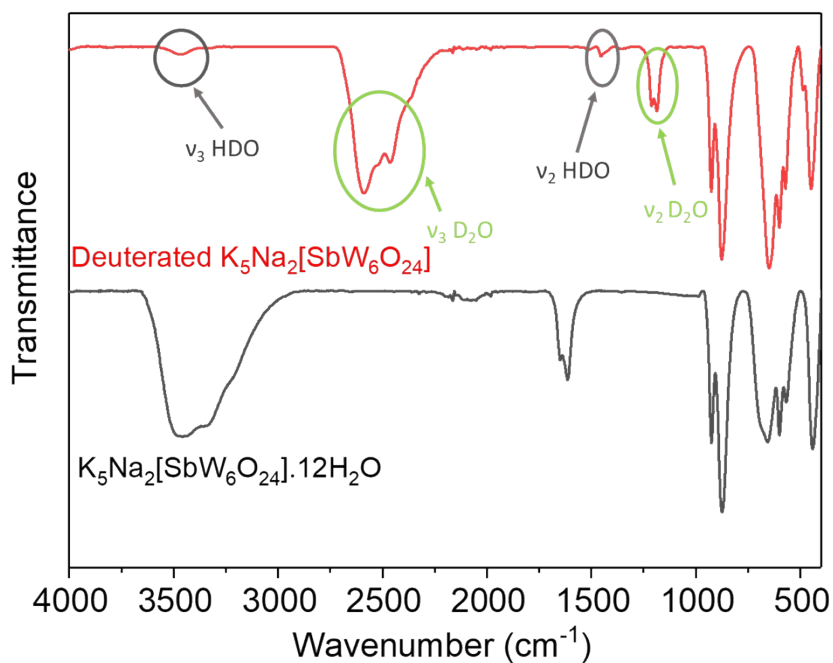


Fig. S18. FTIR-ATR spectra of $\text{K}_5\text{Na}_2[\text{SbW}_6\text{O}_{24}]$ after deuteration (red line) and $\text{K}_5\text{Na}_2[\text{SbW}_6\text{O}_{24}]\cdot 12\text{H}_2\text{O}$ (black line).



The FTIR-ATR spectrum of the deuterated material clearly shows the vibration bands of D_2O around 2500 cm^{-1} (v_3 , OD-stretching modes) and 1200 cm^{-1} (v_2 , DOD-bending modes), together with weakly intense additional bands characteristic of HDO around 1400 cm^{-1} (v_2 , HOD-bending modes) and 3400 cm^{-1} (v_3 , HOD-stretching modes).^{S2} The v_2 HOH-bending modes of H_2O located at about 1600 cm^{-1} in the spectrum of $\text{K}_5\text{Na}_2[\text{SbW}_6\text{O}_{24}]\cdot 12\text{H}_2\text{O}$ are not observed in that of the deuterated sample.

Fig. S19. Absorption spectra of $\text{Na}_7[\text{SbW}_6\text{O}_{24}] \cdot 16\text{H}_2\text{O}$, $\text{Na}_7[\text{SbW}_6\text{O}_{24}]$, $\text{K}_5\text{Na}_2[\text{SbW}_6\text{O}_{24}] \cdot 12\text{H}_2\text{O}$, $\text{K}_5\text{Na}_2[\text{SbW}_6\text{O}_{24}]$, $\text{K}_7[\text{SbW}_6\text{O}_{24}] \cdot 6\text{H}_2\text{O}$ and $\text{K}_7[\text{SbW}_6\text{O}_{24}]$.

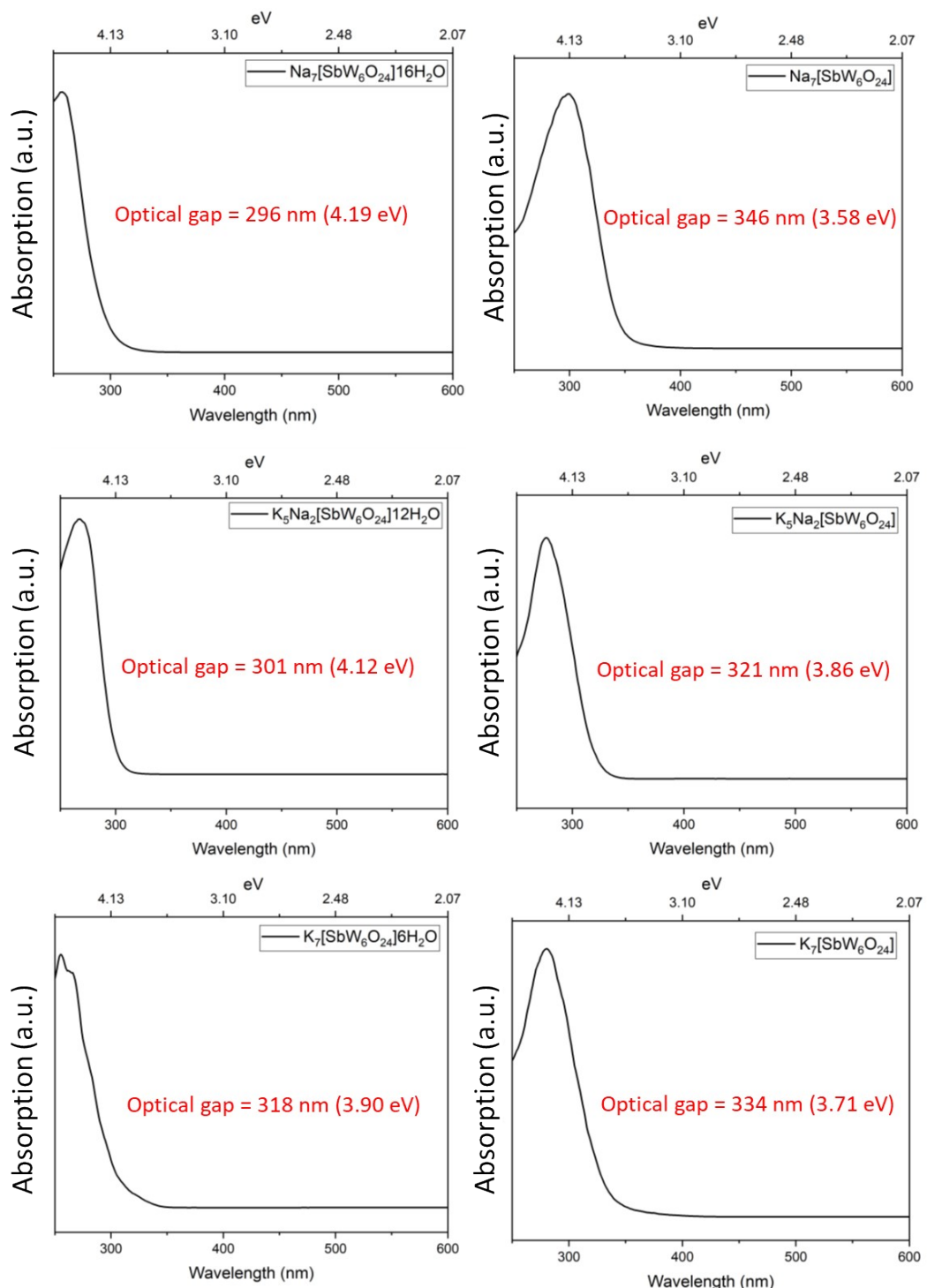


Fig. S20. Room-temperature Excitation spectrum (red line) and emission spectrum (black line) of a) $\text{Na}_7[\text{SbW}_6\text{O}_{24}]\cdot16\text{H}_2\text{O}$, b) $\text{K}_5\text{Na}_2[\text{SbW}_6\text{O}_{24}]\cdot12\text{H}_2\text{O}$, and c) $\text{K}_7[\text{SbW}_6\text{O}_{24}]\cdot6\text{H}_2\text{O}$.

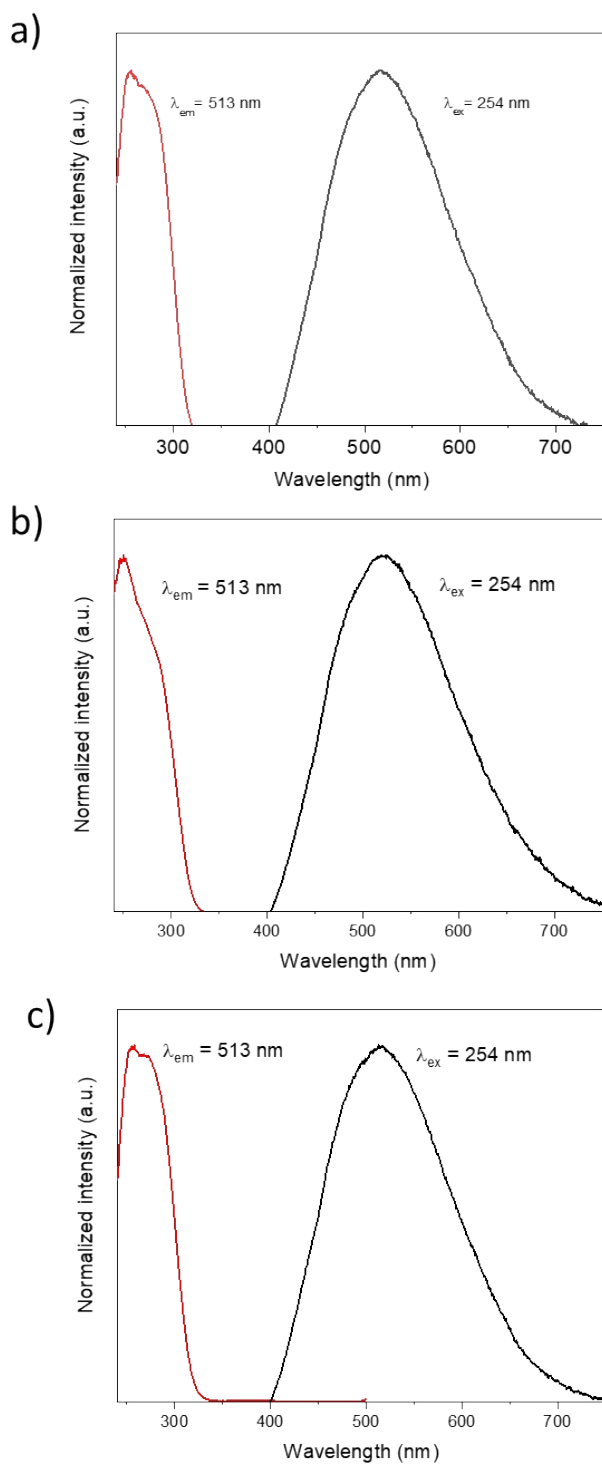


Fig. S21. CIE chromaticity diagrams of $\text{Na}_7[\text{SbW}_6\text{O}_{24}]\cdot16\text{H}_2\text{O}$, $\text{K}_5\text{Na}_2[\text{SbW}_6\text{O}_{24}]\cdot12\text{H}_2\text{O}$ and $\text{K}_7[\text{SbW}_6\text{O}_{24}]\cdot6\text{H}_2\text{O}$ excited at 254 nm.

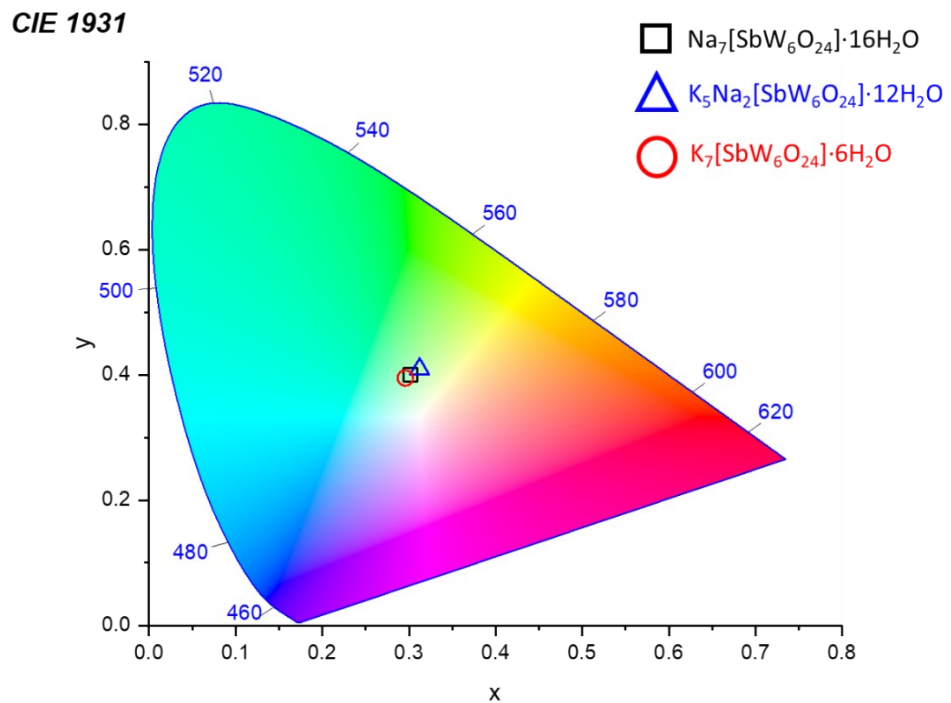


Fig. S22. Room-temperature luminescence decay curves ($\lambda_{\text{ex}} = 254$ nm) monitored at 513 nm for a) $\text{Na}_7[\text{SbW}_6\text{O}_{24}]\cdot16\text{H}_2\text{O}$, b) $\text{K}_7[\text{SbW}_6\text{O}_{24}]\cdot6\text{H}_2\text{O}$, c) $\text{K}_5\text{Na}_2[\text{SbW}_6\text{O}_{24}]\cdot12\text{H}_2\text{O}$, d) $\text{Na}_7[\text{SbW}_6\text{O}_{24}]$, e) $\text{K}_7[\text{SbW}_6\text{O}_{24}]$ and f) $\text{K}_5\text{Na}_2[\text{SbW}_6\text{O}_{24}]$. The plots I = f(t) have been correctly fitted by a monoexponential law. Extracted decay times (τ) and regression coefficients (R^2) are indicated.

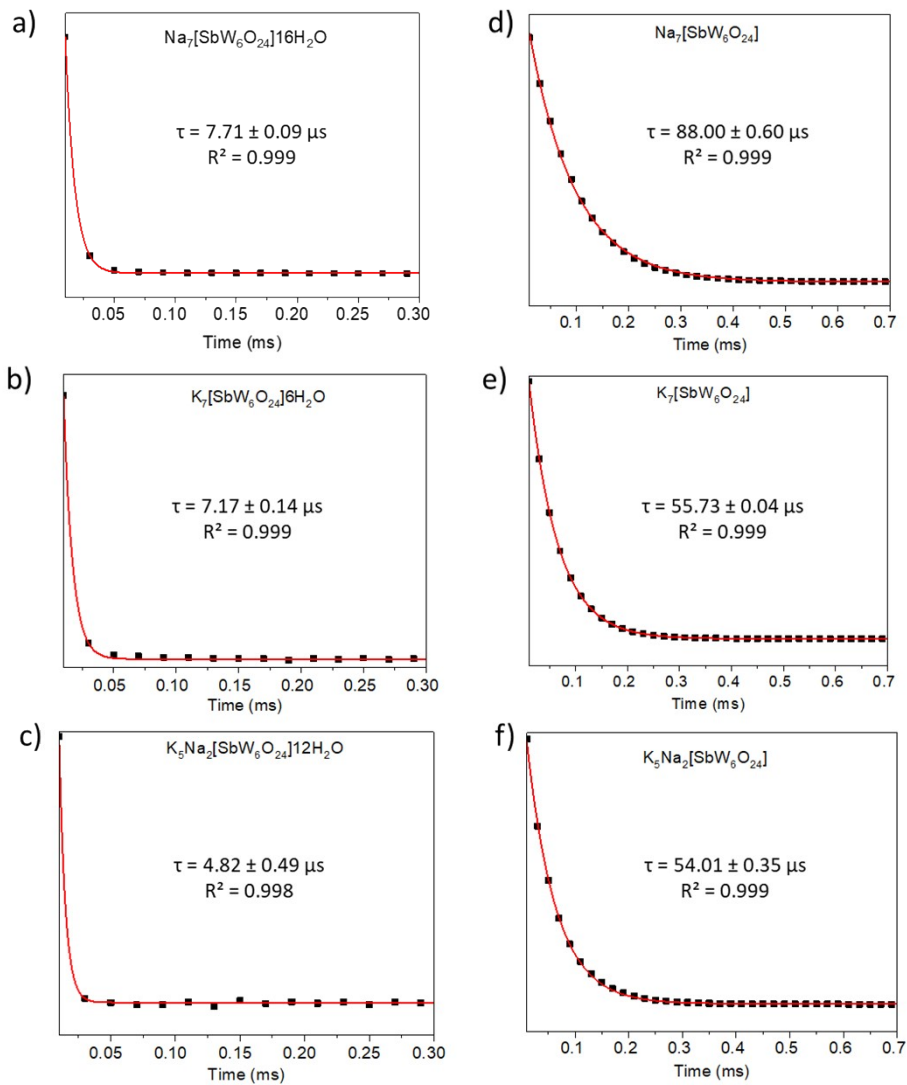


Fig. S23. a) Room-temperature emission spectra monitored at 254 nm of $\text{K}_5\text{Na}_2[\text{SbW}_6\text{O}_{24}]\cdot 12\text{H}_2\text{O}$ (black line) and $\text{K}_5\text{Na}_2[\text{SbW}_6\text{O}_{24}]$ after deuteration in a closed chamber containing heavy water, for five days at room temperature (red line). b) Room-temperature luminescence decay curves ($\lambda_{\text{ex}} = 254$ nm) monitored at 513 nm for $\text{K}_5\text{Na}_2[\text{SbW}_6\text{O}_{24}]$ after deuteration. The plots $I = f(t)$ have been correctly fitted by a monoexponential law. Extracted decay times (τ) and correlation coefficients (R^2) are indicated.

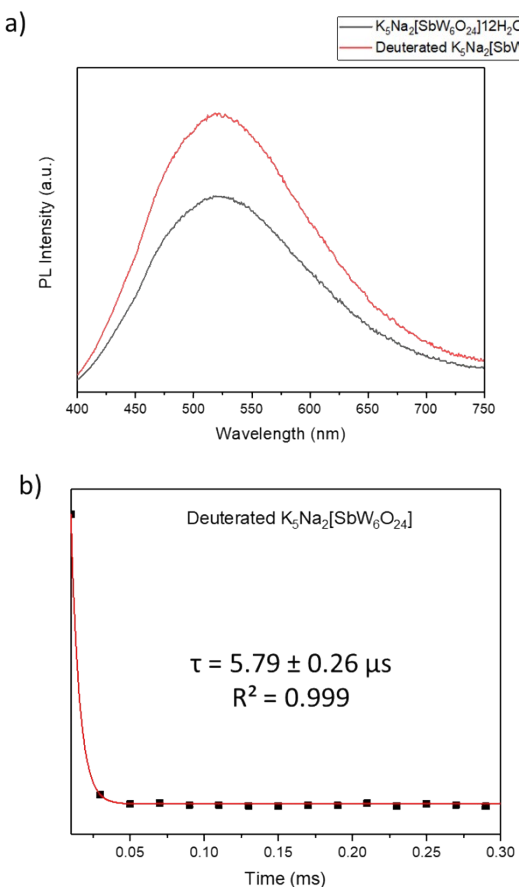


Fig. S24. (a) Top: Photographs of $\text{K}_5\text{Na}_2[\text{SbW}_6\text{O}_{24}]\cdot12\text{H}_2\text{O}$ and $\text{K}_5\text{Na}_2[\text{SbW}_6\text{O}_{24}]$ upon UV excitation ($\lambda_{\text{ex}} = 254 \text{ nm}$) at room temperature. Bottom: Room-temperature excitation spectrum (red line) monitored at 513 nm and emission spectrum (black line) monitored at 254 nm of $\text{K}_5\text{Na}_2[\text{SbW}_6\text{O}_{24}]$. (b) Top: Photographs of $\text{K}_7[\text{SbW}_6\text{O}_{24}]\cdot6\text{H}_2\text{O}$ and $\text{K}_7[\text{SbW}_6\text{O}_{24}]$ upon UV excitation ($\lambda_{\text{ex}} = 254 \text{ nm}$) at room temperature. Bottom: room-temperature excitation spectrum (red line) monitored at 513 nm and emission spectrum (black line) monitored at 254 nm of $\text{K}_7[\text{SbW}_6\text{O}_{24}]$.

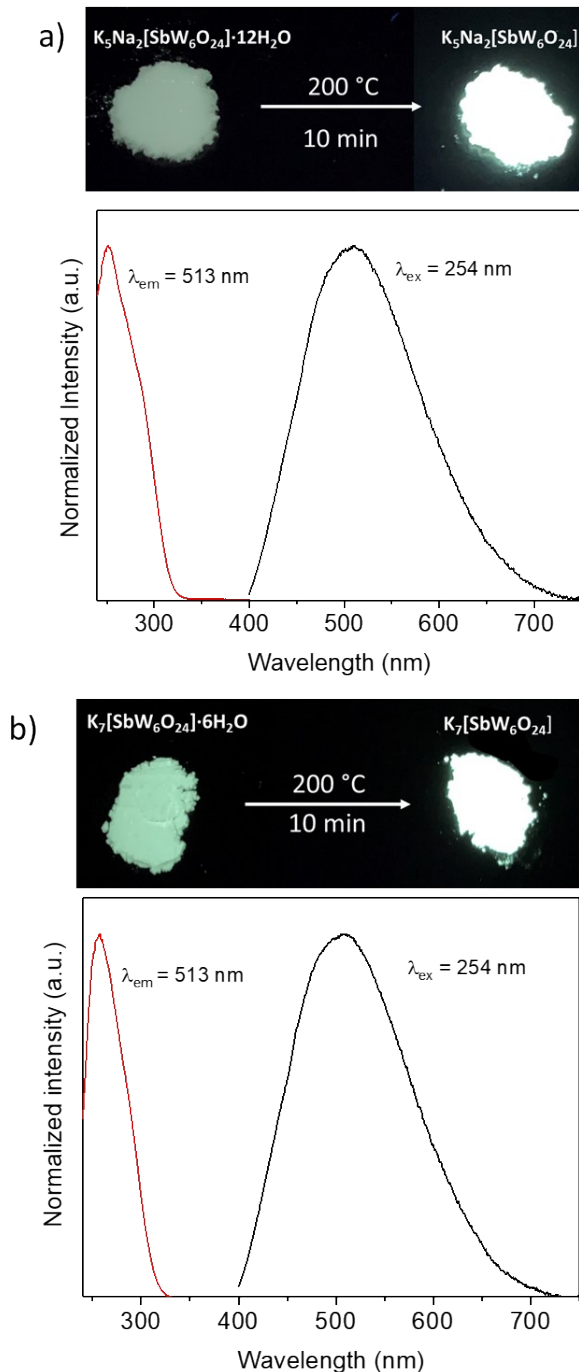


Fig. S25. CIE chromaticity diagrams of $\text{Na}_7[\text{SbW}_6\text{O}_{24}]$, $\text{K}_5\text{Na}_2[\text{SbW}_6\text{O}_{24}]$ and $\text{K}_7[\text{SbW}_6\text{O}_{24}]$ excited at 254 nm.

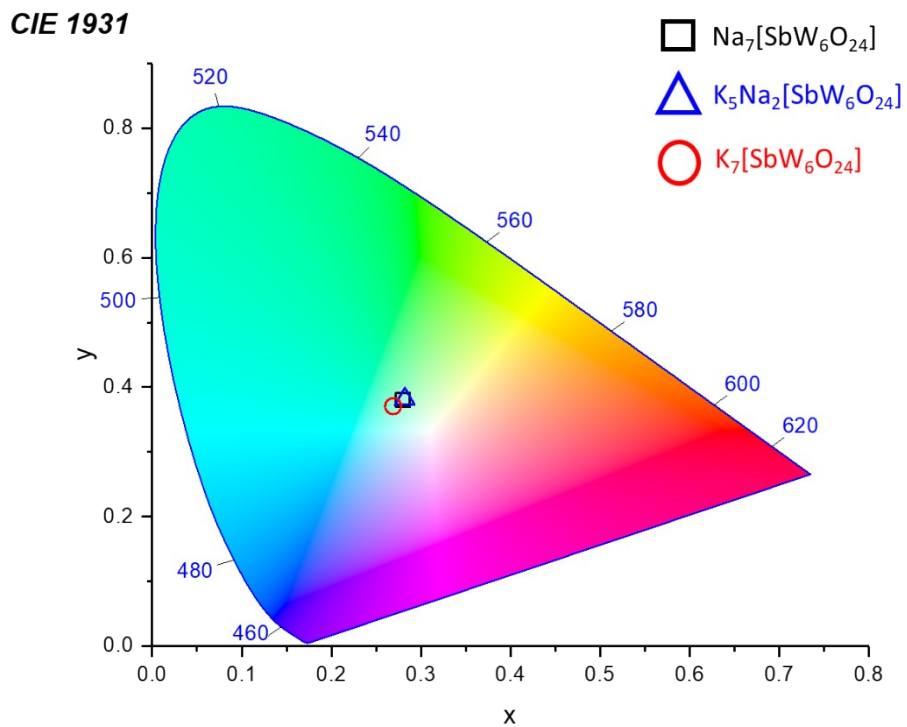


Fig. S26. Room-temperature PL spectra monitored at 254 nm of a) $\text{K}_5\text{Na}_2[\text{SbW}_6\text{O}_{24}]$ and b) $\text{K}_7[\text{SbW}_6\text{O}_{24}]$ before (black line) and after (blue line) rehydration for three days at 100% RH, compared with that of pristine a) $\text{K}_5\text{Na}_2[\text{SbW}_6\text{O}_{24}]\cdot 12\text{H}_2\text{O}$ and b) $\text{K}_7[\text{SbW}_6\text{O}_{24}]\cdot 6\text{H}_2\text{O}$ (red line).

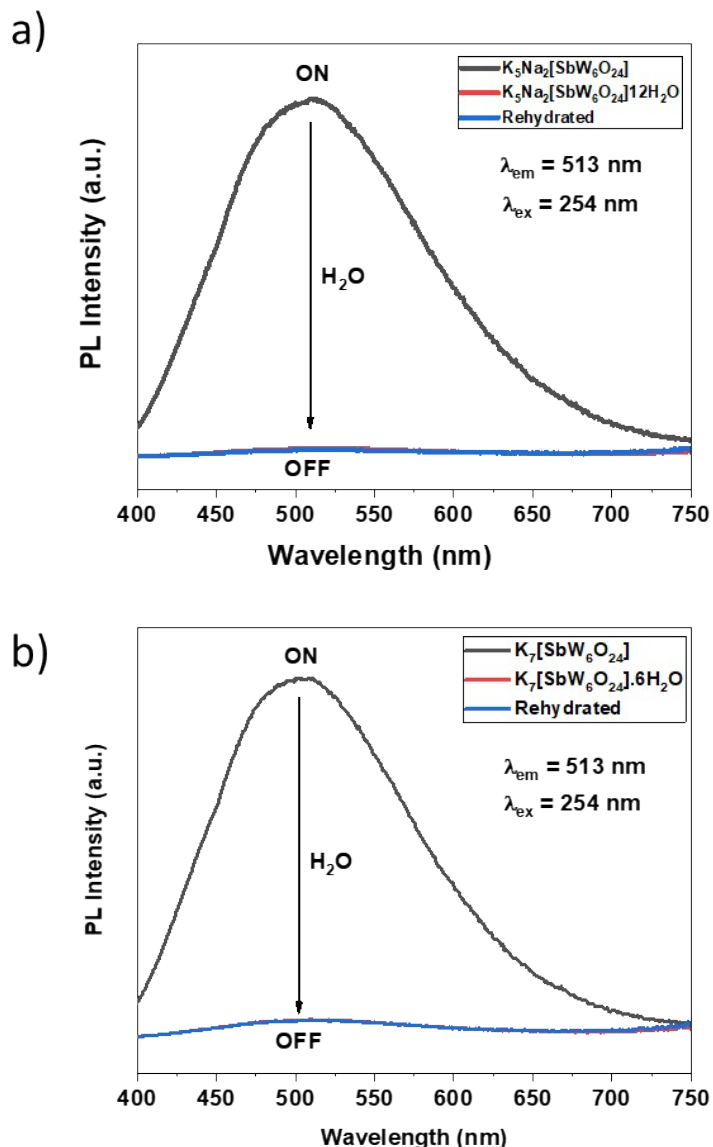


Fig. S27. Evolution of the room-temperature PL spectra (monitored at 254 nm) upon exposure to 100% RH over a period of 480 min for (a) $\text{Na}_7[\text{SbW}_6\text{O}_{24}]$, and over a period of 120 min for (b) $\text{K}_5\text{Na}_2[\text{SbW}_6\text{O}_{24}]$ and (c) $\text{K}_7[\text{SbW}_6\text{O}_{24}]$.

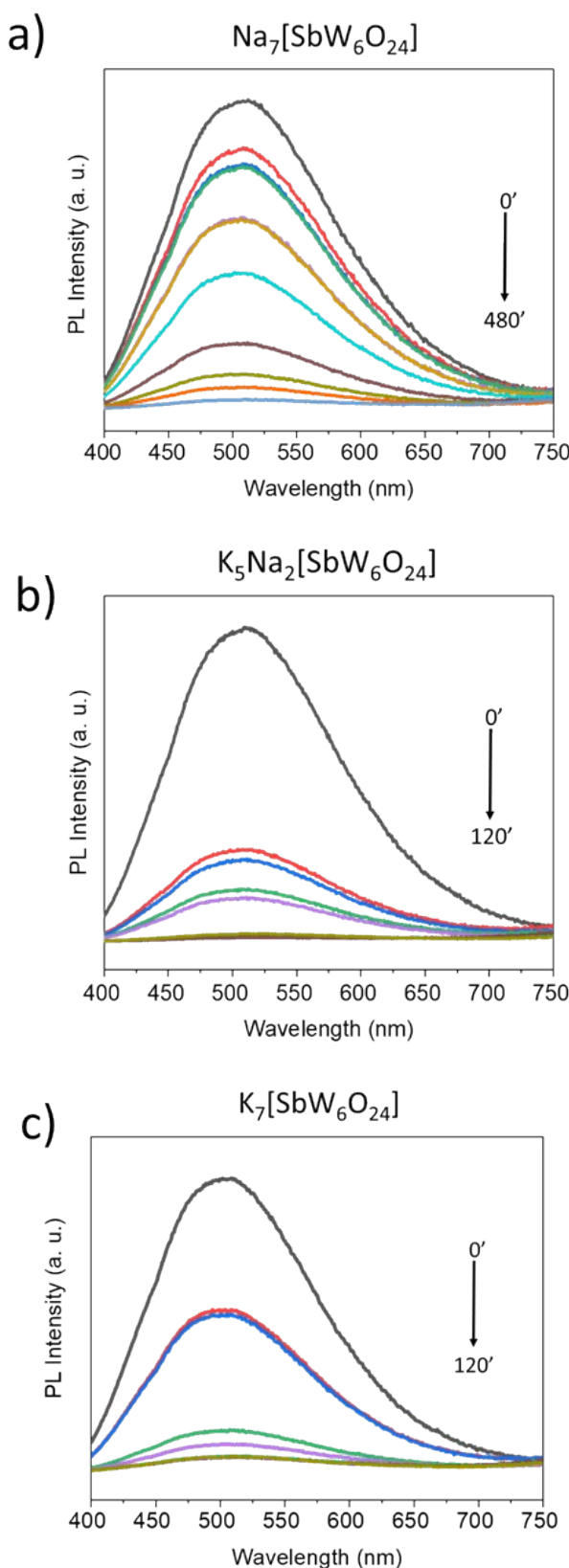
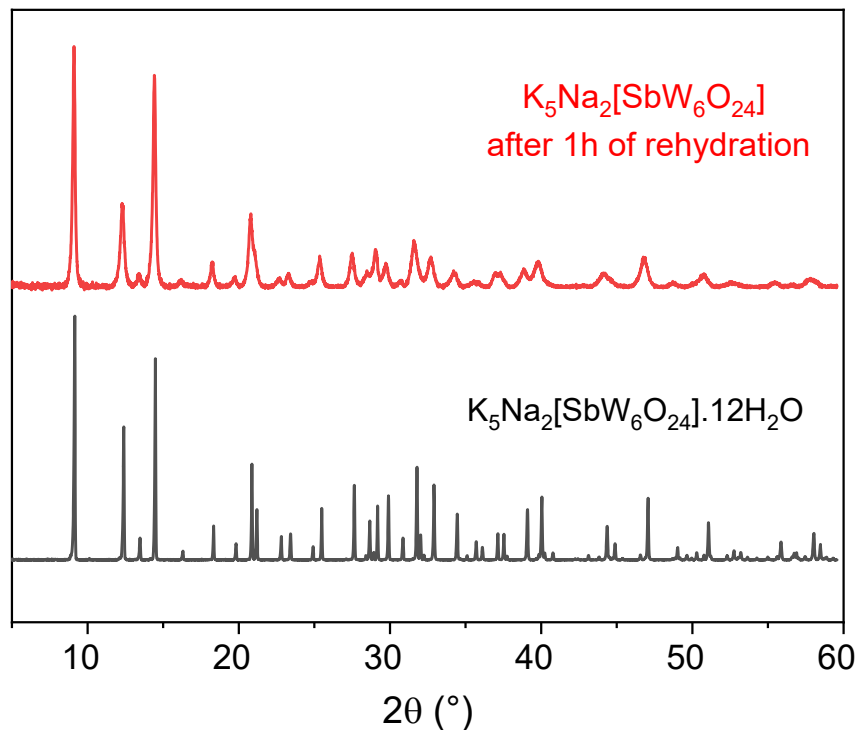


Fig. S28. PXRD patterns of $\text{K}_5\text{Na}_2[\text{SbW}_6\text{O}_{24}]\cdot12\text{H}_2\text{O}$ and $\text{K}_5\text{Na}_2[\text{SbW}_6\text{O}_{24}]$ after rehydration. For the rehydration process, the anhydrous compound was kept for 1h at room temperature in a closed chamber at 100% RH.



References

- S1 H. Naruke, T. Yamase, *Acta Crystallogr. C Cryst. Struct. Commun.* 1992, **48**, 597–599.
S2 M. Ceccaldi, M. Goldman, E. Roth, *Spectrochim. Acta* 1956, **11**, 623–631.